FULL PAPER

Evidence of Oxygen Ferromagnetism in ZnO Based Materials

*Clara Guglieri, Eva Céspedes, Ana Espinosa, María Ángeles Laguna-Marco, Noemi Carmona, Yukiharu Takeda, Tetsuo Okane, Tetsuya Nakamura, Mar García-Hernández, Miguel Ángel García, and Jesús Chaboy**

Discoveries of room-temperature ferromagnetism (RTFM) in semiconductors hold great promise in future spintronics technologies. Unfortunately, this ferromagnetism remains poorly understood and the debate concerning the nature, carrier-mediated versus defect-mediated, of this ferromagnetism in semiconducting oxides is still open. Here, by using X-ray absorption (XAS) and X-ray magnetic circular dichroism (XMCD), it is demonstrated that the oxygen ions have a ferromagnetic response in different ZnO-based compounds showing RTFM behavior: ZnO nanoparticles capped with organic molecules and ZnO/ZnS heterostructures. These results demonstrate the intrinsic occurrence of RTFM in these systems, and point out that it is not related to the metallic cation but it relays on the conduction band of the semiconductor.

1. Introduction

In the past thirteen years, a great deal of effort has been put into the investigation of the mechanisms behind the ferromagnetism in dilute magnetic semiconductors (DMSs), dilute magnetic oxides (DMOs) and even for materials containing no transition-metal impurities, for which a ferromagnetic response persisting up to above room temperature (RTFM) has been reported even when no ferromagnetism was expected at any temperature.[1–6] This interest was triggered by the possibility of combining in a single material the logic functionalities of semiconductors with the information storage capabilities of magnetic elements.

Still, even after more than ten years of intense research, the origin of ferromagnetism in these systems remains a controversial issue from both theoretical[7] and experimental points of view.[1,5,8,9] Most reported evidences of room-temperature ferromagnetism are based on macroscopic magnetometry results. Unfortunately, in many cases, no exhaustive characterization of the materials has been made at the microscopic level so that the ferromagnetism might be likely due to extrinsic effects as magnetic contamination or magnetic secondary-phase formation.[1,5,9,10] It has been also pointed out that this new class of magnetism depends on the structural details of the sample, specially at the near-surface regions (surface, grain boundaries, or interfaces).[11–13] This points the need of using more sophisticated characterization tools able to provide atom-specific magnetic properties and a detailed view of the local structure of the systems under study. The accumulated experience so far dictates the need of using atom-specific structural and magnetic probes as X-ray magnetic circular dichroism (XMCD) and X-ray absorption

C. Guglieri, Dr. M. Á. Laguna-Marco, Dr. J. Chaboy
Instituto de Ciencia de Materiales de Aragón
Consejo Superior de Investigaciones Científicas
– Universidad de Zaragoza
50009, Zaragoza, Spain
E-mail: jchaboy@unizar.es
C. Guglieri, Dr. M. Á. Laguna-Marco, Dr. J. Chaboy
Departamento de Física de la Materia Condensada
Universidad de Zaragoza
50009, Zaragoza, Spain
Dr. E. Céspedes
Institute for Science and Technology in Medicine (ISTM)
Guy Hilton Research Centre
Keele University
Stoke-on-Trent, ST4 7QB, UK
Dr. A. Espinosa
Laboratoire Matière et Systèmes Complexes (MSC)
UMR 7057, Université Paris Diderot
10 rue Alice Domon et Léonie Duquet, 75205, Paris, Cedex 13, France
Dr. N. Carmona
Dpto. Física de Materiales
Universidad Complutense de Madrid
28040, Madrid, Spain
Dr. Y. Takeda, Dr. T. Okane
Condensed Matter Science Division
Japan Atomic Energy Agency
Sayo, Hyogo, 679–5148, Japan
Dr. T. Nakamura
Japan Synchrotron Radiation Research Institute (JASRI/SPring-8)
Sayo, Hyogo, 679–5198, Japan
Prof. M. García-Hernández
Instituto de Ciencia de Materiales de Madrid
CSIC, Cantoblanco, 28049, Madrid, Spain
Dr. M. Á. García
Instituto de Cerámica y Vidrio
CSIC & IMDEA Nanociencia
Cantoblanco, 28049, Madrid, Spain

DOI: 10.1002/adfm.201303087

© 2013 WILEY-VCH Verlag GmbH & Co. KGaA, Weinheim

spectroscopy (XAS) to elucidate the intrinsic nature of the RTFM behavior.[11,14–16]

Application of these advanced tools to the study of Co:ZnO DMOs reveals that the RTFM found in bulk magnetization measurements was not due to Co, whose 3d states show paramagnetic behavior according to XMCD.[14] Similar results were found in the case of Cu-doped ZnO thin films, which display robust room-temperature ferromagnetic signatures using bulk magnetization probes. Keavney and coworkers probed the XMCD at the Cu(3d), O(2p), and Zn(3d) states. They found no dichroic signal consistent with ferromagnetism originating from any of these states: only a paramagnetic component was detected at the Cu(3d), and no magnetic signal in the O or Zn.[17] The experimental findings demonstrate that the 3d electronic shells of the cations in these DMOs do not carry any measurable ferromagnetic moment. This and the observation of ferromagnetism in semiconductor and insulating oxide nanostructures without any doping despite the diamagnetic character of the material in bulk led to a renewed interest in the field.[6,18–20]

Recently, it has been reported that ZnO nanoparticles (NPs) capped with different molecules and showing RTFM behavior, exhibit zero XMCD at the Zn $L_{2,3}$-edges, that is, no magnetic signal stems from the 3d states, whereas Zn K-edge XMCD demonstrated the polarization of the Zn conduction band.[21] The combined analysis of the Zn K-edge XMCD and X-ray absorption near edge structure (XANES) spectra demonstrated the formation of an interface between the ZnO core of the nanoparticle and the organic molecule where this RTFM likely resides.[22] Zn K-edge XMCD measurements reveal the coexistence of two different magnetic contributions: a paramagnetic response from the core of the NP, and a ferromagnetic-like contribution stemming from this interface.[23] The extent and conformation of this interface depends on the capping molecule and, as demonstrated in ZnO/ZnS heterostructures, the FML behavior is reinforced when neat interfaces are formed.[24] These experimental findings are in agreement with the conclusion derived from most theoretical works performed to date, suggesting that magnetism does not result from Zn(3d) orbitals but from the O(2p) orbitals. Indeed, a robust oxygen ferromagnetic state has been predicted even in the absence of magnetic atoms,[25,26] which suggests that the oxygen ions might be responsible for the ferromagnetic moment observed in different ZnO-based compounds. Consequently, the question remaining is to obtain a clear experimental evidence of this RTFM behavior at the anion sublattice.

Here we present the results of X-ray magnetic circular dichroism (XMCD) measurements performed at the O K-edge and at the S K- and L-edges in ZnO nanoparticles capped with organic molecules (dodecylamine and dodecanethiol) and in a $(ZnO_{4\ nm}/ZnS_{4\ nm})_{10}$ heterostructure grown onto Si(100). These systems have already been proved to show room temperature ferromagnetism in macroscopic magnetization measurements,[20–24] in agreement with the magnetic behavior of the Zn conduction band revealed by XMCD measurements at the Zn K-edge. In contrast, no dichroic signal consistent with ferromagnetism originating from the Zn 3d states was previously found. The XANES spectra recorded at both O and S edges reveal the formation of a neat interface. In addition, the O K-edge XMCD evidences the saturation of the element specific magnetic hysteresis measurement (ESMH) magnetization curves while no detectable magnetic signal is found at both the S K-, and L-edges ones. All in all these results demonstrate the intrinsic occurrence of RTFM in these systems and point out that it is not related to the metallic cation but it relays on the conduction band of the semiconductor.

2. Results and Discussion

The O K-edge XAS spectra recorded at room temperature on both AMINE and $(ZnO_{4\ nm}/ZnS_{4\ nm})_{10}$ samples is shown in **Figure 1**. In the case of the AMINE sample, the absorption spectrum is characterized by a broad, asymmetric spectral feature whose maximum lies at ≈ 536.8 eV. This spectral shape is similar to that of bulk ZnO reported in literature although, interestingly, the main absorption peak (peak D in Figure 1) is sharper than in the ZnO case.[15,27] The broad spectral features between 530 and 537 eV are assigned to the transition of O(1s) electrons to the hybridized orbitals of O(2p) and Zn(4s, 4p) states, while the sharp peak at around 537 eV is due to the transition of O(1s) electrons to more localized O $2p_z$ and $2p_{x+y}$ states.[28] The O K-edge XAS does not show any feature related to the O(2p) and Zn(3d) hybridized orbitals as expected for the Zn d^{10} configuration in ZnO. These structures appear in 3d-oxides as sharp peaks in the low energy region (labelled A

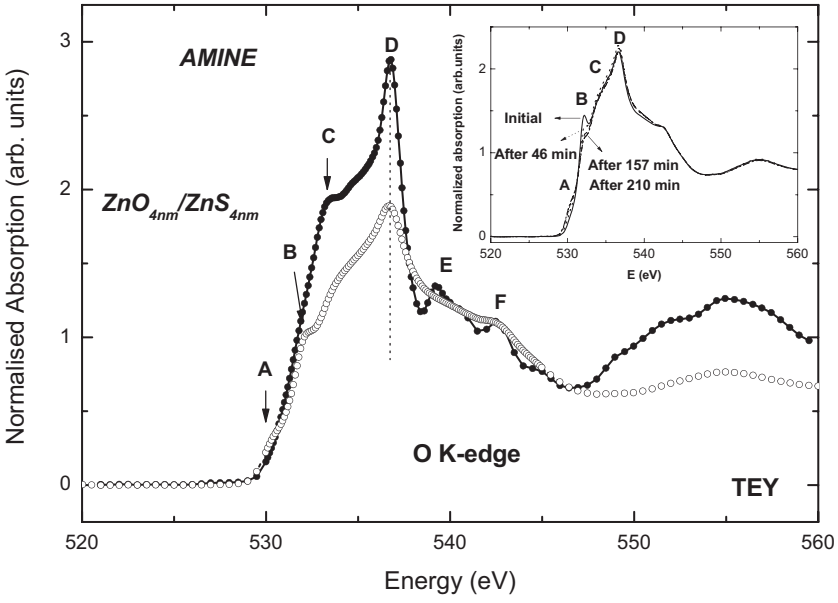

Figure 1. a) Comparison of the room temperature O K-edge XAS spectra of AMINE and $(ZnO_{4\ nm}/ZnS_{4\ nm})_{10}$. The inset shows the changes of the XAS spectra of the heterostructure as a function of the beam exposure.

© 2013 WILEY-VCH Verlag GmbH & Co. KGaA, Weinheim

in the figure) at ~ 530 eV, as illustrated in the case of Co-doped ZnO materials.[29]

The room temperature XAS spectrum of $(ZnO_{4\ nm}/ZnS_{4\ nm})_{10}$ is similar to that of AMINE, although several differences are found. First, there is an overall reduction of the intensity in the region extending from 530 to 540 eV. In addition, a new peak is observed at ≈532.2 eV (B). This peak is only detected in the first scans being disappeared after two hours of exposition to the incoming beam, so that its origin remains controversial. Similar feature has been reported in Cu-doped ZnO thin films, being assigned to the hybridization of O(2p) orbitals with Cu(3d) states,[27] while no peak was observed by Keavney et al. in similar systems.[17] It has been also found in several Co-doped ZnO films and accounted for in terms of oxygen defect states[30] or 3d-O(2p) hybridization.[15,31] However the fact that in some cases this peak is also present in bulk ZnO,[15] and its dependence with the detection method, that is, this peak is only observed for TEY (total electron yield) detection mode and not for TFY (total fluorescence yield), or beam exposure time, casts doubts over these assignments suggesting, on the contrary, that it is due to surface effects.

The most intriguing modification of the XAS spectra occurs, however, when the $(ZnO_{4\ nm}/ZnS_{4\ nm})_{10}$ heterostructure is measured at low temperature (T = 10 K). As shown in **Figure 2** the spectral profile has completely changed with respect to that recorded at room temperature. The characteristic sharp peak of ZnO has been nearly suppressed and, in addition, a new prominent peak (C) arises at ≈533.3 eV. Contrary to the modification of peak B, observed at room temperature, no change of this spectral profile takes place upon long beam exposure time. The energy position of this additional C peak cannot be addressed to contamination by sulfates[32,33] either to the formation of ice.[34,35] Similarly, we ruled out the possibility of the new peaks being caused by preferential orientation effects.[36,37] On the contrary it renders intrinsic to the sample and most likely due to the variation of the electron escape depth in the TEY detection mode.[38] Indeed, the region of the sample probed with this detection method is limited to a depth of a few nm from the surface (≈4 nm) due to inelastic scattering of the secondary electrons.[39] This escape depth is similar to the nominal thickness of the outermost ZnO layer in the heterostructure and, consequently, a small variation can imply that also the ZnO/ZnS interface is being probed. The existence of such a ZnO/ZnS has been previously evidenced by studying the Zn K-edge XANES spectra in these and related systems.[22–24] At this interface, the Zn–O and Zn–S bonding lengths depart from those of the ZnO and ZnS bulk materials. Consequently, if the TEY probes oxygen atoms from both the 4 nm (bulk-like) ZnO layer and from the ZnO/ZnS interface two different O–Zn distances should involved leading to the modification of the O K-edge spectral shape.

Aiming to verify this assignment we have performed a detailed ab-initio calculation of the O K-edge XANES spectra by using the multiple-scattering program CONTINUUM,[40] included in the MXAN program package.[41] A complete discussion of the procedure can be found elsewhere.[22,42] The computation has been performed for a wurtzite-like ZnO (w-ZnO) cluster including the contributions from neighboring atoms located within the first 8 Å around the photoabsorbing

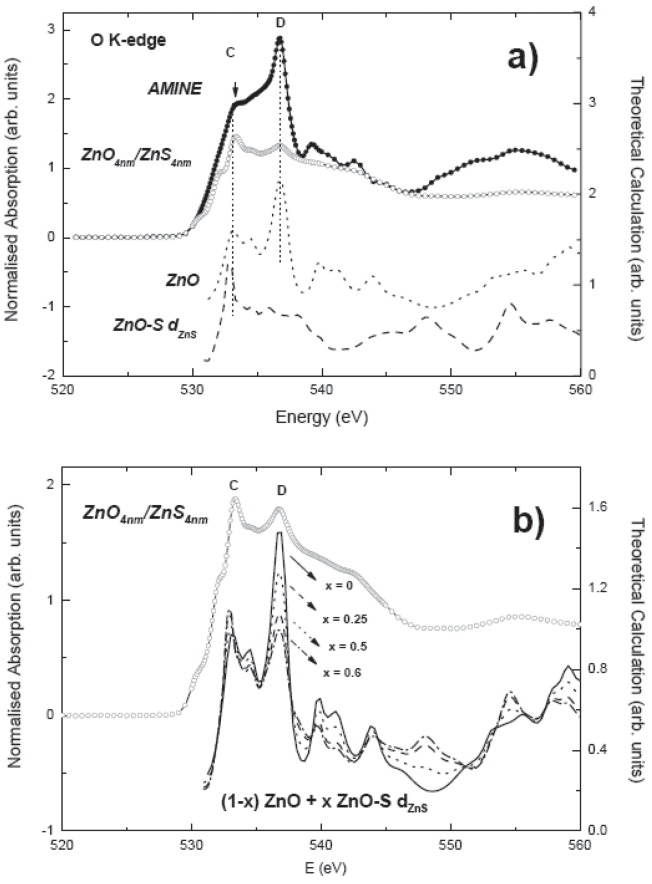

Figure 2. Top: Comparison of the experimental spectra of AMINE and $(ZnO_{4\ nm}/ZnS_{4\ nm})_{10}$ samples recorded at T = 10 K and the computation performed by using a 1% overlapping factor among the muffin-tin spheres and the Dirac-Hara exchange and correlation potential (dashes). The dotted line corresponds to the computation performed by substituting the oxygen atoms of the second coordination shell by sulphur ones and increasing the interatomic O–Zn–S distance as for the ZnS case (see text for details). Bottom: Same comparison as above but weighting both theoretical signals.

oxygen atom. As shown in Figure 2 this calculation reproduces the ZnO O K-edge spectrum. Then, we have proceeded in a second step to evaluate the effect of the proposed Zn–O bond lengthening occurring at the ZnS/ZnO interface to account for the O K-edge XANES measured for the $(ZnO_{4\ nm}/ZnS_{4\ nm})_{10}$ at low temperature. The O–Zn bond length in w-ZnO is 1.98 Å, while the S–Zn one in wurtzite ZnS (w-ZnS) is 2.34 Å. Then, we have considered that upon formation of the aforesaid ZnS/ZnO interface both O and S atoms adapt their interatomic distance to Zn and, as a consequence, the O–Zn bond should be enlarged at this interface. Accordingly, we have performed computations for a ZnO cluster in which the Zn–O bond has been increased to resemble the S–Zn one in ZnS (denoted hereafter as ZnO–S d_{ZnS}). In addition we have also considered the substitution of oxygen atoms in the second coordination shell by sulphur ones in two different arrangements, that is, by maintaining fixed the interatomic distances as for bulk w-ZnO and also by increasing the O–Zn–S interatomic distances as in the case of w-ZnS. The results show that in the later case the peak C, observed for $(ZnO_{4\ nm}/ZnS_{4\ nm})_{10}$

© 2013 WILEY-VCH Verlag GmbH & Co. KGaA, Weinheim

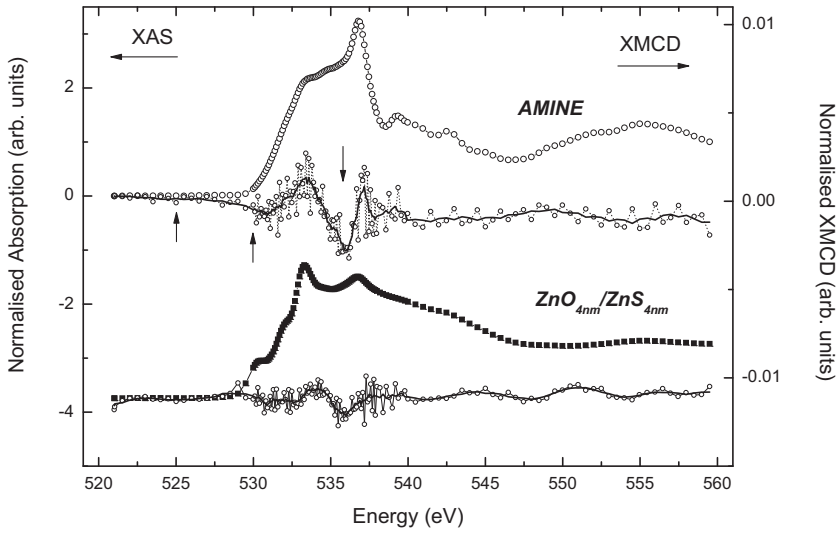

Figure 3. Comparison of the O K-edge XAS and XMCD recorded on AMINE and the $(ZnO_{4\ nm}/ZnS_{4\ nm})_{10}$ samples at $T = 10$ K and $H = 10$ T. The arrows in the XMCD spectrum of AMINE indicates the energy points at which the ESMH measurements have been further performed (see text).

at low temperatures, is reproduced. This validates our interpretation of the origin of this peak in terms of the contribution from the ZnO/ZnS interface. Indeed, the weighted addition of the computations performed for the starting ZnO cluster plus the modified one (recalling that XANES spectrum arises from the averaged contribution of all oxygen atoms of the sample, that is, at the w-ZnO like region and at the interface) in the form $(1 - x)$ZnO + x (ZnO–S d_{ZnS}) shows a remarkably agreement with the experimental spectrum, the best being obtained for $x \approx 50\%$.

The formation of such interface in the case of AMINE, involving N and O atoms, may be also inferred from the differences in the XAS profile of both AMINE and bulk ZnO. However, the expected differences in the Zn-O and Zn-N bond lengths are significantly smaller than in the case of the Zn–S one, which leads to subtle variations in the spectra. In particular, the main difference among the spectra of bulk-ZnO and AMINE resides in the intensity of the white line (peak D), which is appreciably sharper than in the former compound. Thus we have performed similar ab-initio calculation of the O K-edge XANES spectra as detailed above for the heterostructure. The results indicate that the presence of N atoms in the second coordination of the absorbing O atom, that is, the existence of O–Zn–N bonds in the interface between the ZnO core and the capping molecule, enhances the intensity of the main absorption peak (D), in agreement with the experimental observation (see Figure S1 of the Supporting Information).

Beyond the above findings, the most appealing results found in the course of this investigation concern the XMCD measurements. Clear XMCD signals are found at the O K-edge in the case both AMINE and the $(ZnO_{4nm}/ZnS_{4nm})_{10}$ heterostructure (see **Figure 3**). The spectral shape showing two positive peaks at ≈ 533.4 and 537 eV and negative one at ≈ 535.8 eV is similar in both cases. The existence of XMCD at the O K-edge demonstrates the magnetic polarization of the O(2p) orbitals in these ZnO-based systems in the absence of any magnetic (3d) atom. Indeed, the observed O K-edge XMCD clearly differs from that reported by Thakur et al. in MoO_2 thin films.[43] In this case the main XMCD features appears at lower energies, between 530 and 533 eV, as corresponding to the hybridization of the O(2p) and the partially filled 4d orbitals of Mo. The existence of this p-d hybridization in MoO_2 is clearly reflected in the XAS spectral shape contrary to our case where, as discussed above, no signature of O(2p)-Zn(3d) hybridization is found in the O K-edge XAS spectra (see Figure 1). Hence these results give full support to the theoretical predictions of Sanchez et al. on the occurrence of oxygen ferromagnetism in the absence of magnetic atoms.[25] For the sake of completeness we have also recorded the XMCD at the S K-edge in THIOL sample. As shown in **Figure 4** no XMCD signal could be observed in the measured energy region, down to the noise level. Same results have been found at the S L-edges (see Figure S2 in the Supporting Information).

The existence of XMCD at the O K-edge as well as its absence at the S K-edge indicates the magnetic polarization of the O(2p) states, while those of sulphur remain unpolarized.

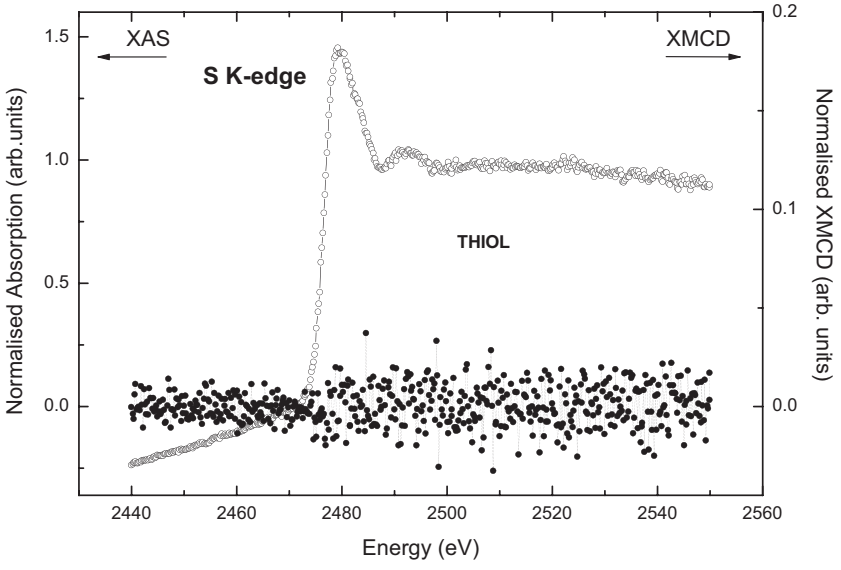

Figure 4. Sulphur K-edge XAS and XMCD spectra recorded at $T = 10$ K and with an applied magnetic field of 5 T in the case of ZnO nanoparticles capped with dodecanethiol (THIOL-3).

© 2013 WILEY-VCH Verlag GmbH & Co. KGaA, Weinheim

These results are in agreement with previous observations on thiol-capped (butanethiol, octanethiol and dodecanethiol) ZnO NPs and ZnS/ZnO heterostructures indicating that ferromagnetism originates at the interface formed between the ZnS shell and the ZnO core, being ferromagnetism favored at those regions of the interface where the local order is closer to w-ZnO than to w-ZnS.[23,24] However, further proof studies are necessary to prove the ferromagnetic character of the magnetic polarization observed at the O K-edge. To this end we have performed element specific magnetic hysteresis (ESMH) measurements. In this experiment, the energy of the photon incoming beam is fixed and the applied magnetic field is varied, which allows monitoring the dependence of the XMCD intensity with the field, $I_{XMCD}(H)$. In contrast to a standard M(H) hysteresis measurement in which the magnetic response is averaged to all the components in the material, the element-specificity of XMCD makes possible to disentangle the magnetic contribution coming from the O(2p) states.[44,45] Then, we have recorded ESMH curves in the case of AMINE fixing the energy at the point in which the XMCD intensity is maximum: 535.8 eV. In addition, we have also recorded the ESMH curves at different points of the spectrum showing no XMCD: 525, 530, and 550 eV, to be used as a reference. The subtraction of the ESMH signals recorded at E = 535.8 eV and at any of these reference points cancels, if present, any spurious signal. The results of these measurements are reported in **Figure 5**. For the sake of completeness we have also applied the same procedure to the ESMH curves measured at different energy reference points (also shown). This comparison yields a clear S-shape dependence of the ESMH curve, in agreement with the occurrence of ferromagnetism arising from the O(2p) states.

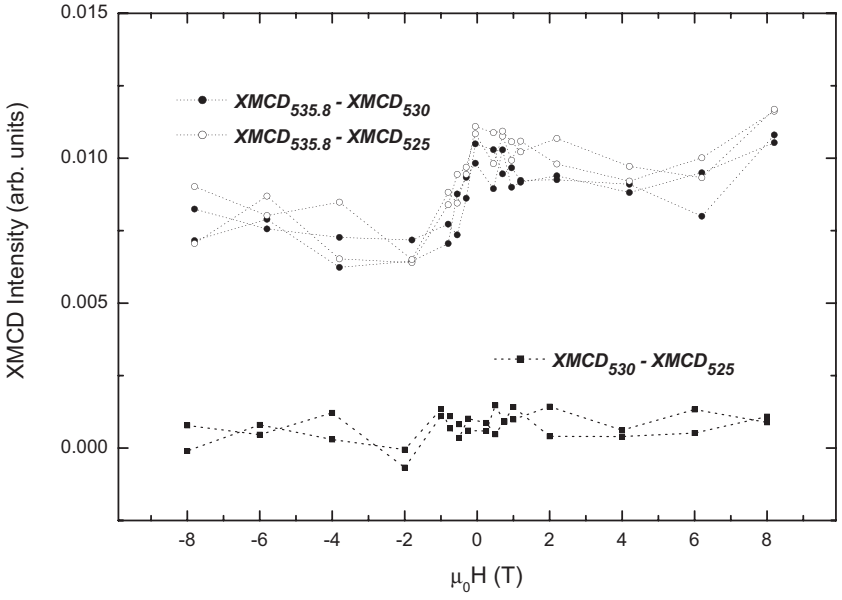

Figure 5. Comparison of the signals obtained from the subtraction of the O K-edge ESMH curves recorded at E = 535.8 eV (highest XMCD intensity) and different reference (zero XMCD) points. The result of applying the same procedure to the curves measured at different energy reference points is also shown. (The signals have been vertically shifted for the sake of clarity, and multiplied by –1 to allow a direct visual comparison with a macroscopic M(H) cycle).

3. Conclusion

In summary, the magnetic properties of ZnO nanoparticles capped with dodecylamine and dodecanethiol, and a $(ZnO_{4\,nm}/ZnS_{4\,nm})_{10}$ heterostructure have been investigated by performing XAS and XMCD measurements at the O K-edge and at the S K- and L-edges. While no appreciable XMCD were observed at the S absorption edges, the O K-edge XMCD shows strong structures and ESMH curves indicative of a ferromagnetic-like magnetic polarization of the O(2p) states. These results demonstrate the intrinsic occurrence of RTFM in these systems and point out that it is not related to the metallic cation (Zn) but it relays on the conduction band of the semiconductor. These results support both theoretical predictions on the occurrence of oxygen ferromagnetic state in the absence of magnetic atoms and the defect-mediated nature of the observed ferromagnetism in these semiconducting oxides.

4. Experimental Section

For these measurements we have used ZnO nanoparticles capped with dodecylamine (hereafter, AMINE), dodecanethiol (hereafter, THIOL) as well as a $(ZnO_{4\,nm}/ZnS_{4\,nm})_{10}$ multilayer film grown onto Si(100). Details of sample preparation and of the structural, optical, and magnetic characterization can be found elsewhere.[20,21,23,24] All the samples show ferromagnetic-like behavior up to room temperature (the magnetization curves show remanence, coercivity (H_C ≈200 Oe), and saturation) whose intrinsic origin has been demonstrated by XMCD experiments performed at the Zn K-edge.[21,23,24]

Both XANES and XMCD spectra were recorded at the oxygen K-edge at the BL23SU beamline of the Japan Atomic Energy Agency (JAEA) in the SPring-8 facility.[46] Left- and right-handed circularly polarized radiation was obtained along the same optical axis by using twin helical undulators. Total electron yield (TEY) measurements were performed at room temperature and at T = 10 K, and the applied magnetic field was varied between 0 and 10 T. Helicity switching using the twin helical undulators has greatly improved the measurement accuracy of XMCD and ESMH. In this way, O K-edge ESMH measurements were performed by fixing the energy of the incoming photons to those energies at which the main features of the XMCD spectra occur. In addition XAS and XMCD were recorded at the S $L_{2,3}$-edges at the BL25SU of the SPring-8 facility.[47,48] Also in this case helicity switching using the twin helical undulators was used to record the XMCD spectra. Measurements were performed at room temperature in ultra high vacuum conditions down to 10^{-8} Pa by the total electron yield (TEY) method. Each XMCD spectrum was taken by reversing the helicity of the incident x-rays while keeping the direction of the magnetic field H = 1.9 T. Finally, Sulphur K-edge XAS and XMCD signals were recorded by using TEY at the 4-ID-C beamline of the APS Facility.[49]

Supporting Information

Supporting Information is available from the Wiley Online Library or from the author.

© 2013 WILEY-VCH Verlag GmbH & Co. KGaA, Weinheim

Acknowledgements

This work was partially supported by Spanish MAT2011–27573-C04–04, MAT2010–16022, CSD2009–00013, MAT2011–27470-C02–02, MAT2010–09346-E, the Madrid Government project NANOBIOMAGNET S2009/MAT-1726, and by the Aragón DGA NETOSHIMA grant. The synchrotron radiation experiments were performed at SPring-8 (Proposal Numbers: 2011B3873, 2011B1700 and 2011B0024) and at APS (Proposal No. GUP-10283). Use of the Advanced Photon Source was supported by the U. S. Department of Energy, Office of Science, Office of Basic Energy Sciences, under Contract No. DE-AC02–06CH11357. The authors acknowledge to J. Freeland for his assistance during the SR experiments at APS. C.G. acknowledges the Ministerio de Educación y Ciencia of Spain for a PhD. Grant. M.A.L.-M. acknowledges to CSIC for a JAE-Doc contract within the Junta para la Ampliación de Estudios program. N.C. acknowledges the financial support of the FSE-MEC, Ramón y Cajal program (ref. RYC-2007–01715). E.C. acknowledges the Ministerio de Educación of Spain for a postdoctoral grant in foreign research centres.

Received: September 4, 2013
Revised: October 17, 2013
Published online: December 2, 2013

[1] S. A. Chambers, *Surf. Sci. Rep.* **2006**, *61*, 345.
[2] S. J. Pearton, W. H. Heo, M. Ivill, D. P. Norton, T. Steiner, *Semicond. Sci. Technol.* **2004**, *19*, R59.
[3] K. Sato, H. Katayama-Yoshida, *Phys. E* **2001**, *10*, 251.
[4] Y. Matsumoto, M. Murakami, T. Shono, T. Hasegawa, T. Fukumura, M. Kawasaki, P. Ahmet, T. Chikyow, S. Koshihara, H. Koinuma, *Science* **2001**, *291*, 854.
[5] J. M. D. Coey, S. A. Chambers, *MRS Bull.* **2008**, *33*, 1053.
[6] K. R. Kittilstved, W. K. Liu, D. R. Gamelin, *Nat. Mater.* **2006**, *5*, 291.
[7] A. Zunger, S. Lany, H. Raebiger, *Physics* **2010**, *3*, 53.
[8] S. Chambers, *Nat. Mater.* **2010**, *9*, 956.
[9] G. Lawes, A. S. Risbud, A. P. Ramírez, R. Seshadri, *Phys. Rev. B* **2005**, *71*, 045201.
[10] M. A. García, E. F. Pinel, J. de la Venta, A. Quesada, V. Bouzas, J. L. Fernández, J. L. Romero, M. S. Martín-González, J. L. Costa-Krämer, *J. Appl. Phys.* **2009**, *105*, 013925.
[11] E. Céspedes, M. A. Laguna-Marco, F. Jiménez-Villacorta, J. Chaboy, R. Boada, C. Guglieri, A. de Andrés, C. Prieto, *J. Phys. Chem. C* **2011**, *115*, 24092.
[12] B. B. Straumal, S. G. Protesova, A. A. Mazilkin, G. Schütz, E. Goering, B. Baretzky, P. B. Straumal, *JETP Lett.* **2013**, *97*, 367.
[13] B. B. Straumal, A. A. Mazilkin, S. G. Protesova, P. B. Straumal, A. A. Myatiev, G. Schütz, E. J. Goering, T. Tietze, B. Baretzky, *Philos. Mag.* **2013**, *93*, 1371.
[14] A. Barla, G. Schmerber, E. Beaurepaire, A. Dinia, H. Bieber, S. Colis, F. Scheurer, J. P. Kappler, P. Imperia, F. Nolting, F. Wilhelm, A. Rogalev, D. Müller, J. J. Grob, *Phys. Rev. B* **2007**, *76*, 125201.
[15] A. P. Singh, R. Kumar, P. Thakur, N. B. Brookes, K. H. Chae, W. K. Choi, *J. Phys.: Condens. Matter* **2009**, *21*, 185005.
[16] T. Tietze, M. Gacic, G. Schütz, G. Jakob, S. Brück, E. Goering, *New J. Phys.* **2008**, *10*, 055009.
[17] D. J. Keavney, D. B. Buchholz, Q. Ma, R. P. H. Chang, *Appl. Phys. Lett.* **2007**, *91*, 012501.
[18] I. Carmeli, G. Leitus, R. Naaman, S. Reich, Z. Vager, *J. Chem. Phys.* **2003**, *118*, 10372.
[19] J. M. D. Coey, M. Venkatesan, C. B. Fitzgerald, *Nat. Mater.* **2005**, *4*, 173.
[20] M. A. García, J. M. Merino, E. Fernández Pinel, A. Quesada, J. de la Venta, M. L. Ruíz-González, G. R. Castro, P. Crespo, J. Llopis, J. M. González-Calbet, A. Hernando, *Nano Lett.* **2007**, *7*, 1489.
[21] J. Chaboy, R. Boada, C. Piquer, M. A. Laguna-Marco, M. García-Hernández, N. Carmona, J. Llopis, M. L. Ruíz-González, J. González-Calbet, J. F. Fernández, M. A. García, *Phys. Rev. B* **2010**, *82*, 064411.
[22] C. Guglieri, J. Chaboy, *J. Phys. Chem. C* **2010**, *114*, 19629.
[23] C. Guglieri, M. A. Laguna-Marco, M. A. García, N. Carmona, E. Céspedes, M. García-Hernández, A. Espinosa, J. Chaboy, *J. Phys. Chem. C* **2012**, *116*, 6608.
[24] C. Guglieri, A. Espinosa, N. Carmona, M. A. Laguna-Marco, E. Céspedes, M. L. Ruíz-González, M. González- Calbet, M. García-Hernández, M. A. García, J. Chaboy, *J. Phys. Chem. C* **2013**, *117*, 12199.
[25] N. Sánchez, S. Gallego, M. C. Muñoz, *Phys. Rev. Lett.* **2008**, *101*, 067206.
[26] A. Espinosa, N. Sánchez, J. Sánchez-Marcos, A. de Andrés, M. C. Muñoz, *J. Phys. Chem. C* **2011**, *115*, 24054.
[27] P. Thakur, V. Bisogni, J. C. Cezar, N. B. Brookes, G. Ghiringhelli, S. Gautam, K. H. Chae, M. Subramanian, R. Jayavel, K. Asokan, *J. Appl. Phys.* **2010**, *107*, 103915.
[28] J. Chen, *Surf. Sci. Rep.* **1997**, *30*, 1.
[29] S. Kumar, Y. J. Kim, B. H. Koo, H. Choi, C. G. Lee, S. K. Sharma, M. Knobel, S. Gautam, K. H. Chae, *J. Korean Phys. Soc.* **2009**, *55*, 1060.
[30] S. Krishnamurthy, C. McGuinness, L. S. Dorneles, M. Venkatesan, J. M. D. Coey, J. G. Lunney, C. H. Patterson, K. E. Smith, T. Learmonth, P. A. Glans, T. Schmitt, J.-H. Guo, *J. Appl. Phys.* **2006**, *99*, 08M111.
[31] Z. Sun, W. Yan, G. Zhang, H. Oyanagi, Z. Wu, Q. Liu, W. Wu, T. Shi, Z. Pan, P. Xu, S. Wei, *Phys. Rev. B* **2008**, *77*, 245208.
[32] N. Pangher, L. Wilde, M. Polcik, J. Haase, *Surf. Sci.* **1997**, *372*, 211.
[33] E. Todd, D. Sherman, J. Purton, *Geochim. Cosmochim. Acta* **2003**, *67*, 881.
[34] A. Nilsson, D. Nordlund, I. Waluyo, N. Huang, H. Ogasawara, S. Kaya, U. Bergmann, L.-A. Näslund, H. Öström, Ph.Wernet, K. J. Andersson, T. Schiros, L.G.M. Pettersson, *J. Electron Spectrsc. Relat. Phenom.* **2010**, *177*, 99.
[35] S. Myneni, Y. Luo, L. Å. Näslund, M. Cavalleri, L. Ojamäe, H. Ogasawara, A. Pelmenschikov, P. Wernet, P. Väterlein, C. Heske, Z. Hussain, L. G. M. Pettersson, A. Nilsson, *J. Phys.: Condens. Matter* **2002**, *14*, L213.
[36] J.-H. Guo, L. Vayssieres, C. Persson, R. Ahuja, B. Johansson, J. Nordgren, *J. Phys.: Condens. Matter* **2002**, *14*, 6969.
[37] J. W. Chiou, J. C. Jan, H. M. Tsai, C. W. Bao, W. F. Pong, M.-H. Tsai, I.-H. Hong, R. Klauser, J. F. Lee, J. J. Wu, S. C. Liu, *Appl. Phys. Lett.* **2004**, *84*, 3462.
[38] E. J. Sternglass, *Phys. Rev.* **1957**, *108*, 1.
[39] F. de Groot, A. Kotani, *Core Level Spectroscopy of Solids*, Taylor & Francis, London, **2008**.
[40] C. R. Natoli, D. R. Misemer, S. Doniach, F. W. Kutzler, *Phys. Rev. A* **1980**, *22*, 1104.
[41] M. Benfatto, S. D. Longa, *J. Synchrotron Radiat.* **2001**, *8*, 1087.
[42] C. Guglieri, E. Céspedes, C. Prieto, J. Chaboy, *J. Phys.: Condens. Matter* **2011**, *23*, 206006.
[43] P. Thakur, J. C. Cezar, N. B. Brookes, R. J. Choudhary, R. Prakash, D. M. Phase, K. H. Chae, R. Kumar, *Appl. Phys. Lett.* **2009**, *94*, 062501.
[44] C. T. Chen, Y. U. Idzerda, H.-J. Lin, G. Meigs, A. Chaiken, G. A. Prinz, G. H. Ho, *Phys. Rev. B* **1993**, *48*, 642.

© 2013 WILEY-VCH Verlag GmbH & Co. KGaA, Weinheim

[45] Strictly speaking, O K-edge absorption probes the empty p-states projected on the absorbing site. Thus, even when the main contribution is expected to come from the O(2p) states, the Zn-sp states should be also concerned due to the hybridization at the conduction band.
[46] Y. Saitoh, Y. Fukuda, Y. Takeda, H. Yamagami, S. Takahashi, Y. Asano, T. Hara, K. Shirasawa, M. Takeuchi, T. Tanaka, H. Kitamura, *J. Synchrotron Radiat.* **2012**, *19*, 388.
[47] Y. Saitoh, H. Kimura, Y. Suzuki, T. Nakatani, T. Matsushita, T. Muro, T. Miyahara, M. Fujisawa, K. Soda, S. Ueda, H. Harada, M. Kotsugi, A. Sekiyama, S. Suga, *Rev. Sci. Instrum.* **2000**, *71*, 3254.
[48] T. Nakamura, T. Muro, F. Guo, T. Matsushita, T.Wakita, 7 T. Hirono, Y. Takeuchi, K. Kobayashi, *J. Electron Spectrsc. Relat. Phenom.* **2005**, *144–147*, 1035.
[49] J. W. Freeland, J. C. Lang, G. Srajer, R. Winarski, D. Shu, D. M. Mills, *Rev. Sci. Instrum.* **2002**, *73*, 1408.

© 2013 WILEY-VCH Verlag GmbH & Co. KGaA, Weinheim